Applied Physics A (2021) 127:101
https://doi.org/10.1007/s00339-020-04258-y

Applied Physics A
Materials Science & Processing

Facile synthesis of CuO nanostructures for non-enzymatic glucose sensor by modified SILAR method

A. S. Patil[1] · R. T. Patil[2] · G. M. Lohar[3] · Vijay J. Fulari[2]

Received: 21 July 2020 / Accepted: 26 December 2020 / Published online: 13 January 2021

Abstract

The authors developed CuO nanorice, using a modified SILAR method for non-enzymatic glucose sensing. The copper oxide was deposited onto the substrate of stainless steel and distinguished by various characterization techniques. A monoclinic structure that is substantially functional for enzyme less glucose sensors have been deposited with polycrystalline CuO. The rice-like morphology of CuO confirms FE-SEM. The electrochemical efficiency of CuO electrodes is calculated by the adoption of cyclic voltammetry (CV) and chronoamperometry (CA) in a 0.1 M NaOH solution with a potential of + 0.6 V (vs. Ag/AgCl). This sensor offers a linear response from 0 to 3 mM to glucose concentration and has a sensitivity of 1017 μAmM^{-1} cm^{-2}.

Keywords Copper oxide · m-SILAR · Non-enzymatic glucose sensor · Cyclic voltammetry · Chronoamperometry

1 Introduction

Glucose detection is essential for the modern era as well as it is an important task in modern human life. It includes the food industry, pharmaceutical industry, environmental monitoring. According to the clinical field, the development of glucose sensors is paying great attention [1]. The usual range of glucose concentration in human blood is 4–8 mM. If it exceeds, the patient experiences diabetes mellitus. Also, they experience severe impediments like blindness, heart, and kidney failure [2, 3]. For the monitoring of glucose, many electrochemical methods are widely used in various research fields because they possess unique advantages like simplicity, sensitivity, and better cost, selectivity as well as detection [4]. All glucose sensors are grouped with enzyme and without enzyme. The enzymes show intrinsic behaviour hence enzymatic sensor having poor stability. Also, the pH of a solution, moisture, temperature, and hazardous chemicals rigorously affects the enzyme activity [5]. Usually, for enzymatic glucose sensors, glucose oxidase (GO) enzyme is used because it is more stable, but glucose sensors based on GO suffer instability, poor reproducibility, poor stability, and complicated immobilization procedure, thermal and chemical deformation [6]. Hence, it is important to develop and modify glucose sensors that are economical, highly selective, and trustworthy. The transition metal oxide like Co_3O_4 [7], CuO [8], NiO [9], Fe_2O_3 [10] shows high stability, low cost, improved oxidation of glucose. Amid, CuO is an emerging material to glucose sensors because it has high catalytic activity, excellent durability, environmentally friendliness, and the ability to promote electron transfer [11, 12]. The cupric oxide (CuO) is abundantly available in nature. Its synthesis is cost-effective [13]. It shows properties like nontoxicity, excellent chemical stability, good electrochemical activity, large surface area [14]. It shows stability in different solutions and air also [15].

For the deposition of CuO various physical or chemical methods have been used, like sol–gel [16], CVD [17], electrodeposition [18], thermal oxidation [19], sputtering [20], successive ionic layer adsorption and reaction (SILAR) [21], and spray pyrolysis [22]. Amid, the SILAR, is more effective because it is suitable at low temperatures, a cost-effective solution method. Also, it helps to mass production, to control thickness and phase purity over composition. Also,

✉ Vijay J. Fulari
vijayfulari@gmail.com

[1] Rajarshi Chhatrapati Shahu College, Kolhapur 416005, Maharashtra, India

[2] Holography and Materials Research Laboratory, Department of Physics, Shivaji University, Kolhapur 416004, Maharashtra, India

[3] Lal Bahadur Shastri College of Arts, Science and Commerce, Satara 415002, Maharashtra, India

the properties of CuO can be modified by varying deposition time and deposition cycles [15]. Guanghua et al. [23] synthesized ultrathin CuO nanowire arrays on copper oxide wire with the help of heat treatment. The prepared CuO has 850.7 μAmM^{-1} cm^{-2} of sensitivity. Zang et al. [24] fabricated CuO nanowires by a chemical method, which demonstrated a sensitivity of 648 μAmM^{-1} cm^{-2}. Yang et al. [25] developed CuO nanoleaves and decorated with carbon nanotube by a chemical precipitation method, with a sensitivity of 664.3 μAmM^{-1} cm^{-2}. Yang et al. [26] synthesized CuO nanoparticles and decorated them with N-doped graphene aerogel. The method used is hydrothermal. The prepared electrode achieves a sensitivity of 223.1 μAmM^{-1} cm^{-2}.

Herein, Polycrystalline, rice-like CuO electrodes are developed using a cost-effective and simple modified SILAR (m-SILAR) method. The prepared electrode was characterized to study the different properties of copper oxide. The rice-like CuO is used for glucose sensors. For glucose sensing, especially cyclic voltammetry and chronoamperometry were employed in 0.1 M NaOH. This electrode was utilized for amperometric study to the analysis of enzymeless glucose sensing performance. The prepared CuO nanostructures show a sensitivity of 1017 μAmM^{-1} cm^{-2} towards glucose.

2 Experimental details

2.1 Synthesis of CuO thin films

CuO was deposited on stainless steel as substrates using the m-SILAR technique for the production of the CuO electrode. The cationic solution was prepared using sodium thiosulphate ($Na_2S_2O_3$) as a solvent for the synthesis of the CuO electrode and copper sulphate pentahydrate ($CuSO_4.5H_2O$) as a solvent. $Na_2S_2O_3$ was injected drop by drop into the 0.1 M copper sulphate pentahydrate ($CuSO_4.5H_2O$) to obtain a cationic solution to create a cationic solution until the resulting solution becomes colourless. This consequent solution is referred to as a complex solution. 100 ml of a complex solution is used as a source for cations. And 100 ml of 0.1 M sodium hydroxide (NaOH) kept at 343 K, as a source of an anionic solution.

Stainless steel (1 cm × 5 cm) substrates were carefully washed with ultrasonic treatment. m-SILAR cycles were typically initiated with the aid of the substrate holder by dipping the stainless steel substrate into an anionic solution for 5 precious seconds. Consequently, substrates were dipped into the complex solution that serves as the source of cations for 5 s. In this way one m-SILAR cycle was properly executed. The deposition of the substrate takes place on both sides. Normal and repeated immersions have been carried out for up to 160 cycles. The films were eventually inserted for rinsing purposes in double-distilled water and then air-dried.

The CuO electrodes were prepared for 130, 140, 150, 160 deposition cycles and named as a:130 repetitions, b:140 repetitions, c:150 repetitions,d:160 repetitions. The prepared samples were air-dried at 623 K for one hour to improve the crystalline structure. It has been observed that the lateral thickness of electrodes of CuO increases with the number of m-SILAR repetitions to 160 repetitions. As m-SILAR cycles increase the thickness of the films increases, dislocation density and microstrain decreases, more defects are generated in the film that reduces crystallite size [27]. As microstrain decreases stress on film increases, resulting in the film being peeled out the film after reaching beyond optimum thickness. In present work, film being peeled out after 160 cycles. In chemically deposited films, the peeling of film material is common and is mainly due to the relatively poor adhesion [28].

2.2 Characterizations

The structural properties of the CuO electrode were analysed by XRD diffractometer with a Bruker D2 phaser tabletop model with copper radiation (Cu-Kα, λ = 1.5406 Å). The molecular structure was confirmed by Thermo Nicolet, Avatar 370 FT-IR spectrometer. The surface morphological and compositional study was done by FE-SEM and EDS of Mira-3, Tescan Pvt, Brno-Czech Republic. The electrochemical biosensing measurements were carried out using the electrochemical workstation CH608E. The electrochemical system contains three-electrodes, CuO electrode—working electrode, platinum—counter electrode, and Ag/AgCl—reference electrode and 0.1 M NaOH solutions the electrolyte.

3 Result and discussion

3.1 XRD Studies

The XRD study of CuO electrodes concerning different deposition cycles onto stainless steel substrates shown in Fig. 1. From XRD analysis**,** it is clear that deposited samples exhibit distinct peaks that indicate polycrystalline nature. The peaks (002), (111), (-313) readily identifies the monoclinic phase was confirmed by JCPDS card 00-002-1040 [29, 30]. The observed and standard "*d*" values are nearly equal and shown in Table 1. The lattice parameters are $a = 4.65$ Å, $b = 3.41$ Å, $c = 5.10$ Å. The calculation of crystallite size (D) is done by applying the Scherrer formula [31, 32] and is mentioned in Table 1. Due to ion by ion deposition in the m-SILAR method number of cations (cu^+) and anions (OH^-) increases, this increases electrode thickness. As a result of this, crystallite size increases with deposition cycles. Some

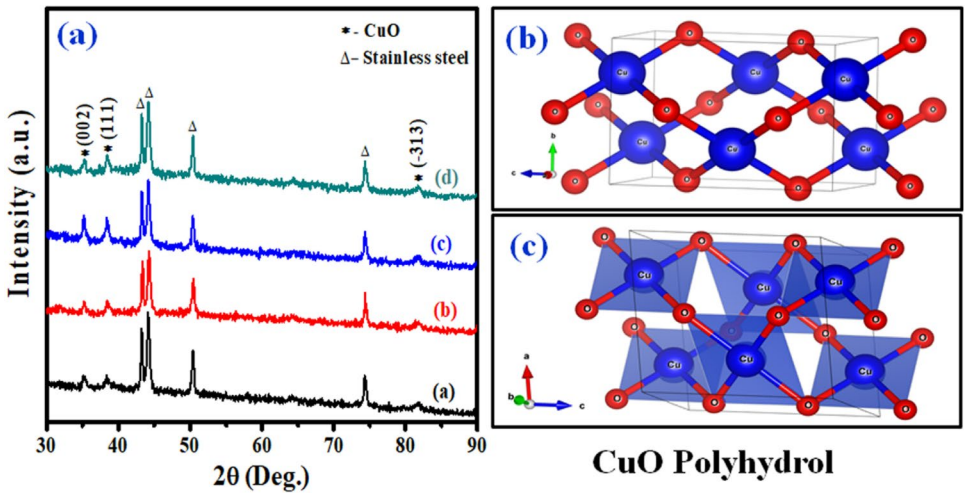

Fig. 1 The XRD patterns of CuO with **a** 130 cycles **b** 140 cycles **c** 150 cycles **d** 160 cycles

Table 1 Observed and Standard parameters from XRD study

Sr. no	No. of m-SILAR cycles	2θ (Deg.)	Observed "*d*"	Standard "*d*"	D (nm)
1	130	35.21	2.54	2.52	13.27
		38.50	2.33	2.32	
2	140	35.17	2.55	2.52	15.49
		38.46	2.340	2.32	
3	150	35.16	2.55	2.52	17.72
		38.46	2.34	2.32	
4	160	35.17	2.55	2.52	14.31
		38.44	2.34	2.32	

peaks belong to Cu-OH at XRD and these peaks are created due to air moisture.

3.2 FT-IR Studies

FT-IR spectra of CuO electrodes deposited with the m-SILAR method are displayed in Fig. 2 and are used to get structural information of CuO. The main peaks were obtained at 1631, 1386, 1120, 1000, 605, 501 cm^{-1}. The stretching of copper and oxygen in CuO was observed at 1000–610 cm^{-1} [33, 34]. The peaks around at 1120, 1386, and 1631 cm^{-1} belong to Cu-OH bending vibrations. The frequency obtained at 502 and 601 cm^{-1} indicates vibrations due to stretching in monoclinic CuO. The Cu–O stretching along (022) direction was observed at 605 cm^{-1} and the frequencies at 501 cm^{-1} representing the Cu–O stretching beside (111) [35, 36]. Thus FT-IR analysis suggests the presence of CuO having a monoclinic structure. At FT-IR, some peaks belong to Cu-OH and these peaks are formed and observed at 1631 cm^{-1} due to air moisture. FT-IR study also reveals the presence

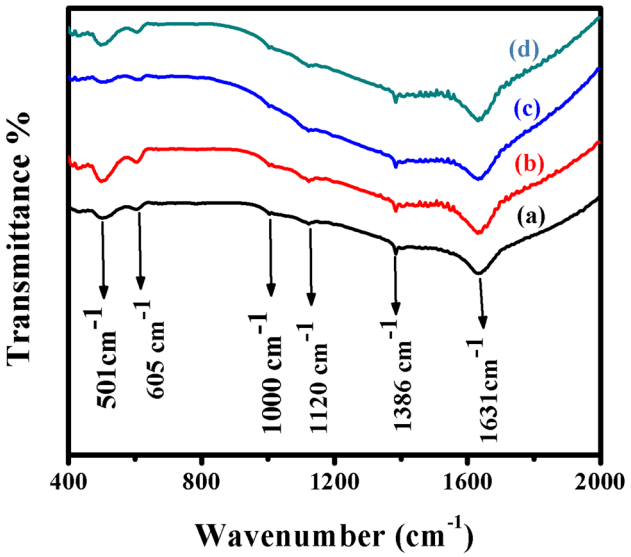

Fig. 2 The FT-IR patterns of CuO with **a** 130 cycles **b** 140 cycles **c** 150 cycles **d** 160 cycles

of a few constitutional water molecules incorporated in the CuO. Thus, it confirms the formation of copper oxide compounds.

3.3 FE-SEM Studies

The surface morphology of CuO deposited at various m-SILAR deposition cycles annealed at 623 K was studied by FE-SEM. Moreover, the FE-SEM images are demonstrated in Fig. 3a–d. From the FE-SEM study, it was observed that deposited CuO exhibits rice like morphology [37]. The CuO nanorice deposited at 130 m-SILAR cycles, nanorice having a length of 310 nm, and a width of 40 nm. Also, CuO at 140 m-SILAR cycles having a length of 370 nm and a width of 90 nm. The CuO at 160 deposition

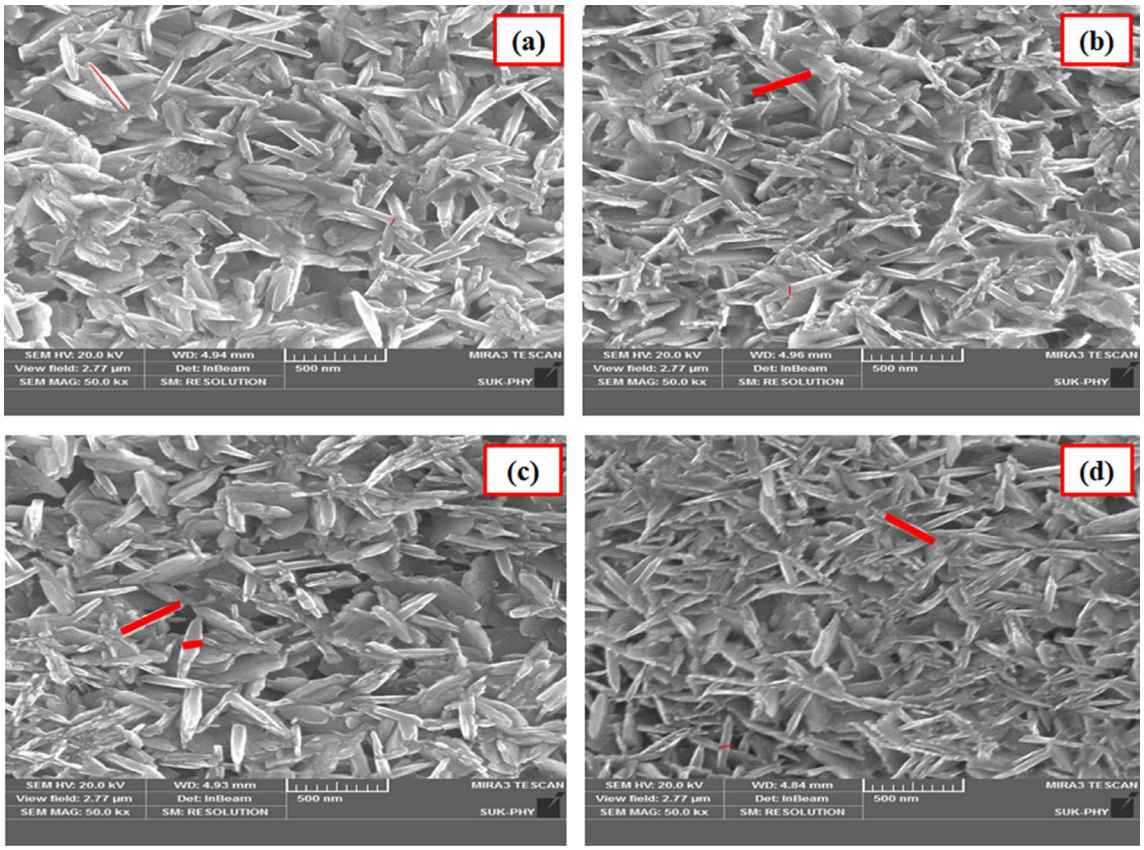

Fig. 3 The FE-SEM images of CuO with **a** 130 cycles **b** 140 cycles **c** 150 cycles **d** 160 cycles

cycles, CuO exhibits a length of 280 nm and a width of 50 nm. The m-SILAR deposition cycles increases, grain size was observed to increases. For 140 deposition cycles, CuO grain exhibits 320 nm length and 50 nm width. Such type of morphology produces the porous volume, which develops the structural foundation for the biosensing performance [38].

3.4 EDS Studies

Figure 4a–d represents typical EDS patterns of the CuO with different m-SILAR deposition cycles and its detailed analysis. The sharp peaks corresponding to the characteristic emission of X-rays by Cu and O are visible, which confirm the formation of CuO without any elemental impurities. The elemental analysis for Cu and O was carried out, and the average atomic percentage is mentioned in Table 2. Table 2 having information about an atomic percentage copper and oxygen present in CuO, and both are nearly equal. Moreover, the peaks observed in EDS images are the substrate material peaks.

3.5 Cyclic voltammetry study

The CV was employed to study the sensitivity of glucose. The prepared CuO electrodes (a, b, c, d) were employed as glucose sensing anodes with different concentrations (0–3 mM) at various scan rates of 10, 20, 50, and 100 mVs^{-1} as shown in Fig. 5. In these cyclic voltagramms, no redox peaks were observed; however, at 0.6 V vs. Ag/AgCl, observed a gradual decrease in current due to the addition of NaOH [39]. Because of the good surface area, enhanced electron transfer ability, great surface energy, there is an excellent improvement in the performance of electrodes a, b, and c, which increases the electrocatalytic ability of electrodes towards glucose oxidation [40]. Equation 1 and Eq. 2 represent the mechanisms of oxidation of glucose mentioned in [41].$CuO + OH^- \leftrightarrow CuOOH + e^-$

$$CuOOH + e^- + \text{glucose} \leftrightarrow CuO + OH^- + \text{gluconicacid} \quad (1)$$

$$CuOOH + e^- + \text{glucose} \leftrightarrow CuO + OH^- + \text{gluconicacid} \quad (2)$$

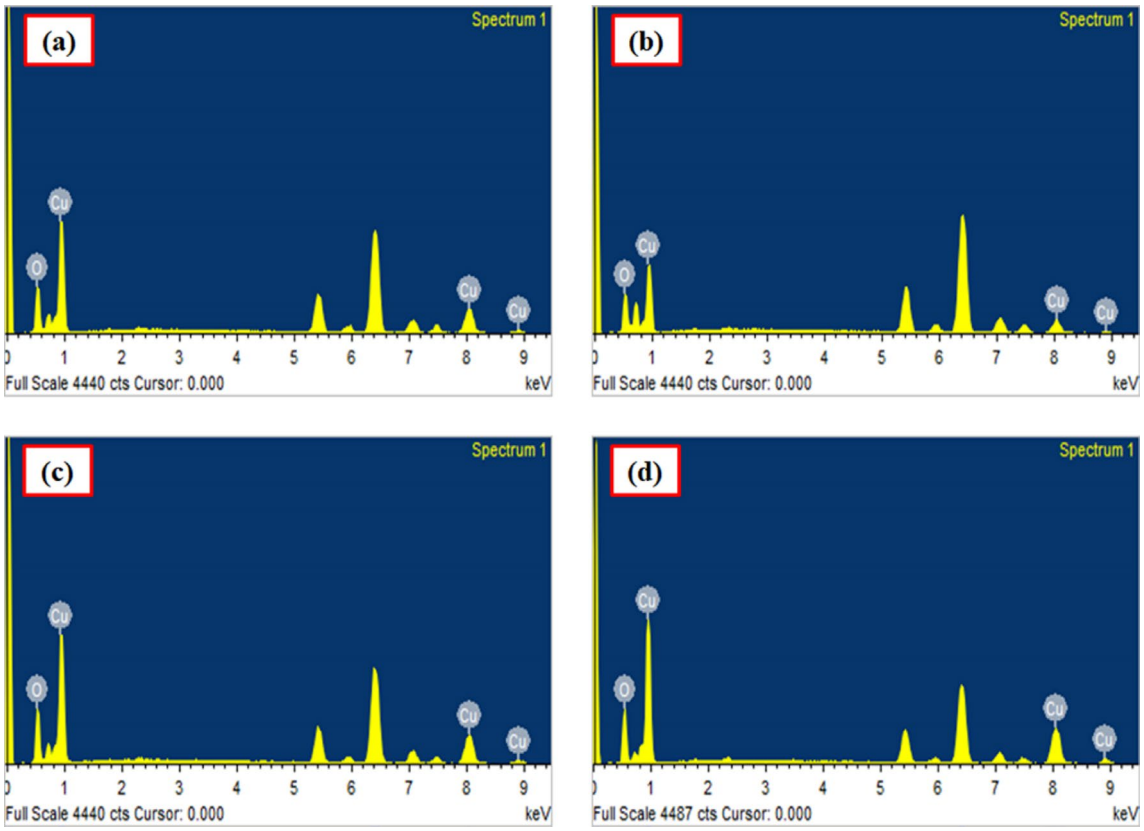

Fig. 4 The EDS spectra of CuO with **a** 130 cycles **b** 140 cycles **c** 150 cycles **d** 160 cycles

Table 2 Compositional percentage of CuO thin films deposited at various deposition cycles

Sr. no	No. of cycles	Atomic %	
		Copper	Oxygen
1	130	49.76	50.24
2	140	47.49	52.61
3	150	49.80	50.20
4	160	47.75	52.25

While performing these chemical reactions, electrons were produced during the oxidation of glucose. And these electrons were transferred to the working electrode. That leads to the enhancement in current, which intimates the excellent catalytic properties of CuO.

3.6 Chronoamperometry (CA) Study

For the detection of glucose, the chronoamperometry technique was used. For this, 0.5 mM glucose at the interval of 50 s was added to the electrolyte. The + 0.6Vvs. Ag/AgCl, a potential applied to study chronoamperometry and the results were made known in Fig. 6. As glucose concentration increases, the increase in current was observed with steps like nature [42].

3.7 Sensitivity

Figure 7 shows a graph of current versus glucose concentration. The sensitivity calculations were done using active area, calibration curve, and slope [43]. As expected from CV data electrode a, b, c, exhibits sensitivity in the ascending order, and for '*d*' electrode sensitivity decrease. The sensitivities of respected electrodes and corresponding *R*-squared values (correction coefficients) are mentioned in Table 3.

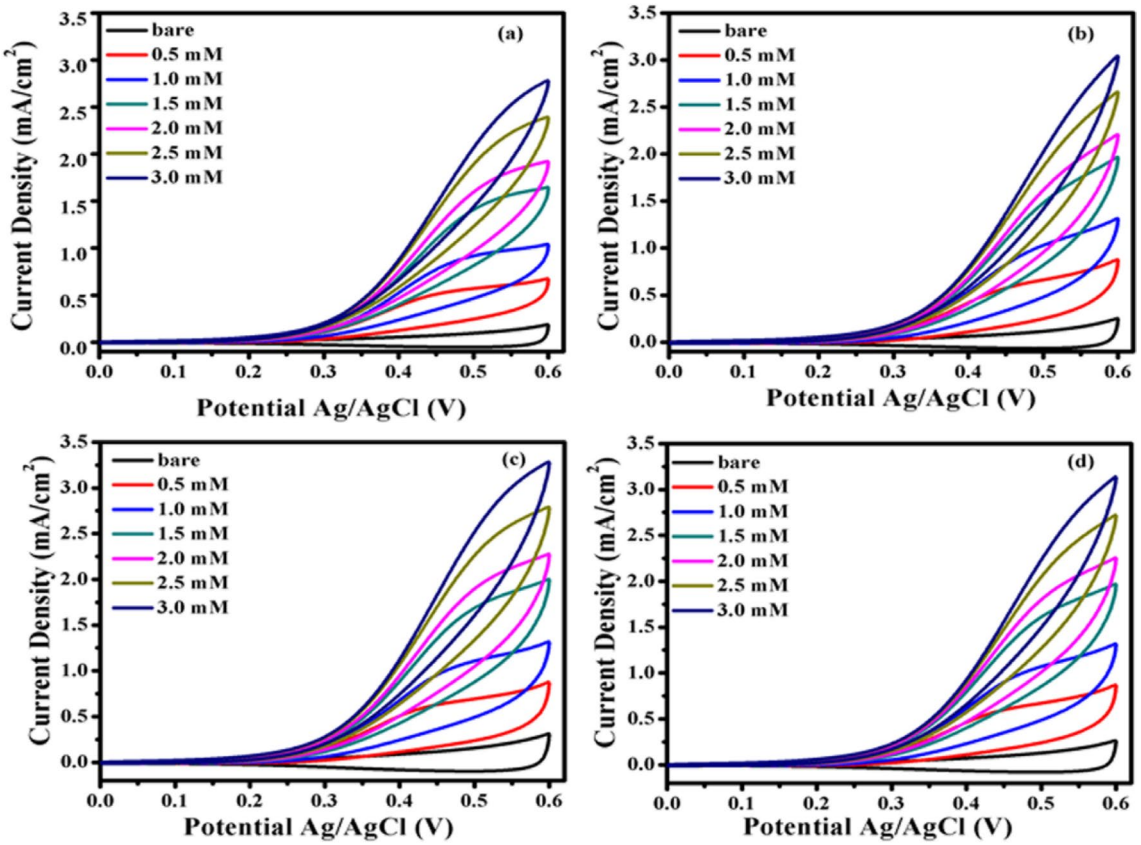

Fig. 5 The cyclic voltagramms of CuO with **a** 130 cycles **b** 140 cycles **c** 150 cycles **d** 160 cycles at 50 mV scan rate

3.8 Selectivity

Many interfering species are extant in blood with glucose. Here, we studied the selectivity of prepared electrodes towards ascorbic acid (AA) which generally co-exist in blood along with glucose. The literature survey suggests the AA having 30 times less concentrations in human blood as compared to glucose [44]. While performing chronoamperometry along with 0.5 mM glucose, 0.05 mM AA was added successively with the interval of 50 s in 30 ml 0.1 M NaOH at the potential of + 0.6 V.The current–time graphs are mentioned in Fig. 8. Simultaneous addition of 0.05 mM of ascorbic acid (AA) along with 0.5 mM glucose does not show any important response from the sensor. The spikes for glucose indicate good selectivity of the CuO electrode towards glucose. Also, the present work confirms CuO is having good selectivity and useful for real blood sample analysis.

4 Conclusions

In summary, CuO electrodes synthesized using the m-SILAR method is easy to synthesis and binder-free. The deposition cycles influence the kinetics of the reaction; also, it alters the crystallinity, morphology, and electrochemical sensing performance of CuO. The CuO has a monoclinic

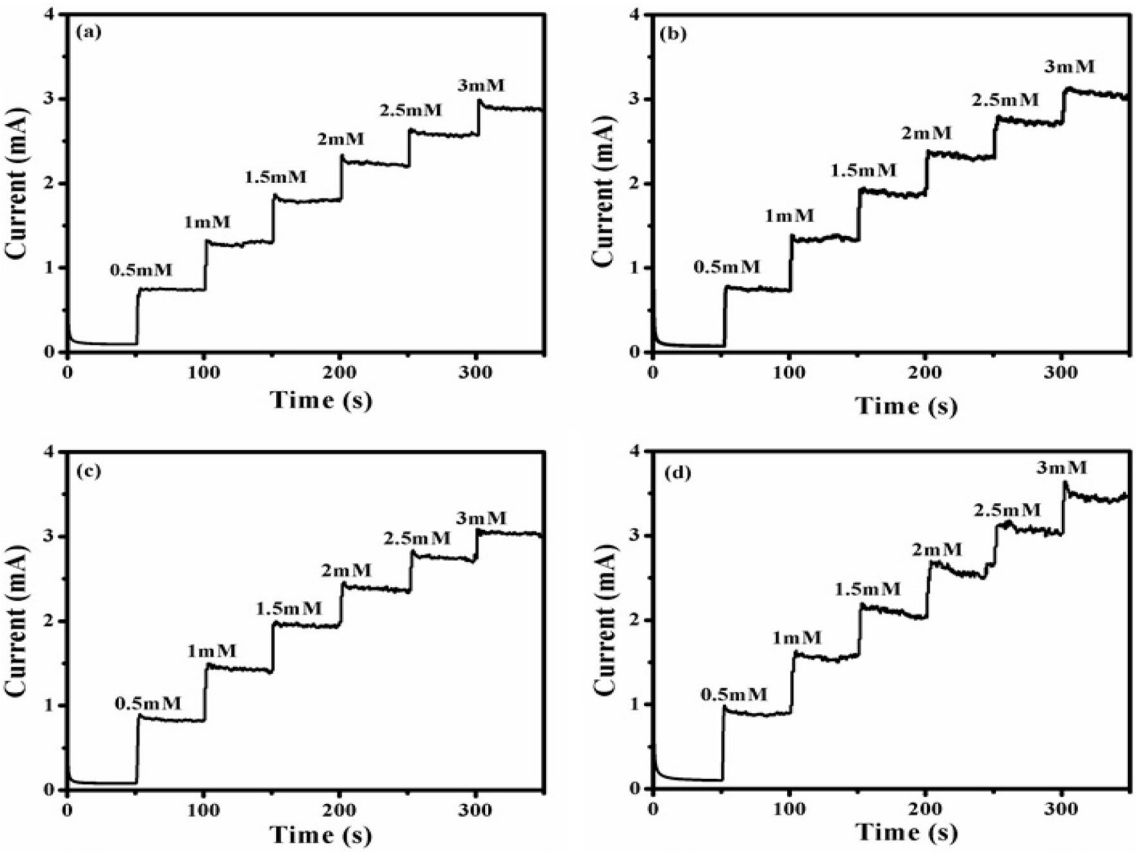

Fig. 6 The amperometric response curves of CuO with **a** 130 cycles **b** 140 cycles **c** 150 cycles **d** 160 cycles at 50 mV scan rate

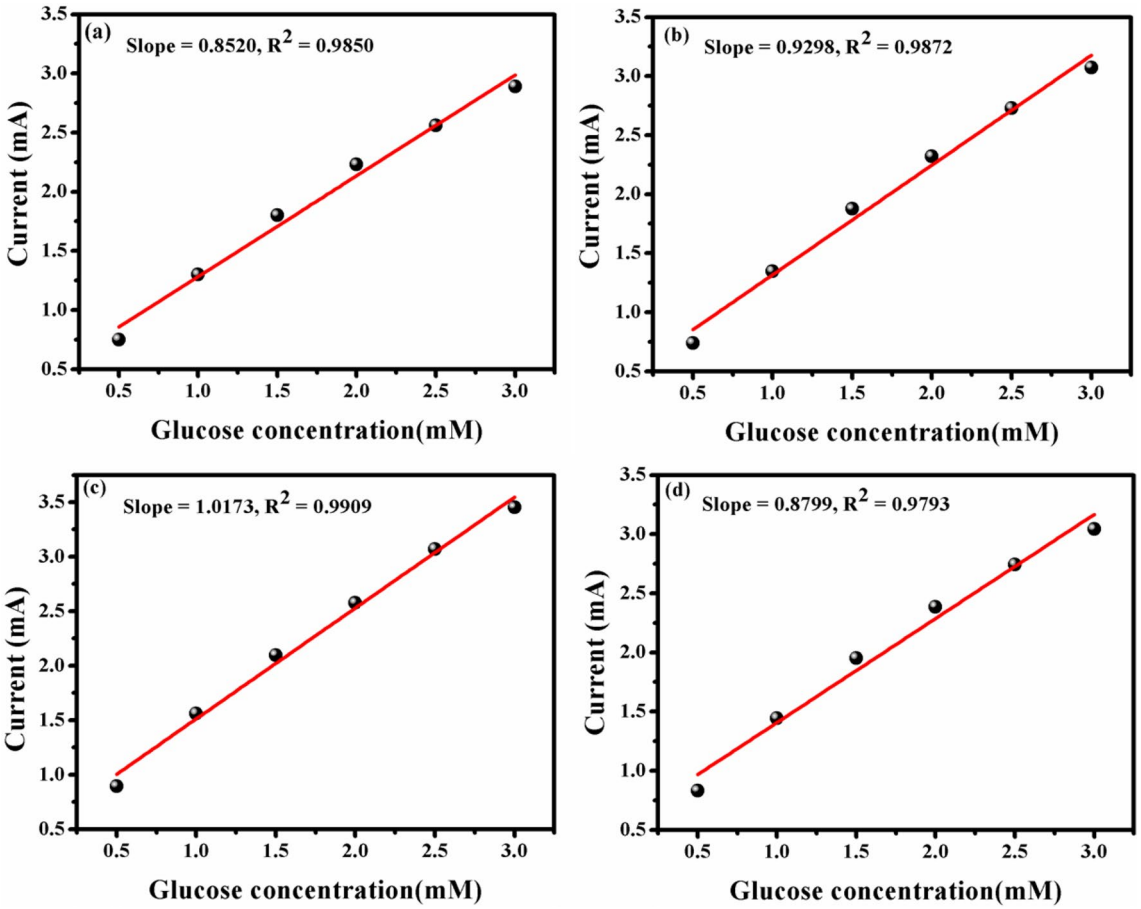

Fig.7 The calibration curves of CuO with **a** 130 cycles **b** 140 cycles **c** 150 cycles **d** 160 cycles

Table 3 Sensitivity and R^2 values of prepared CuO thin films at different deposition cycles

Sr. no	No. of m-SILAR deposition cycles	Sensitivity ($\mu AmM^{-1}\ cm^{-2}$)	*R*-squared value
1	130	852	0.98
2	140	929	0.98
3	150	1017	0.99
4	160	879	0.97

structure and rice like morphology. The electrochemical measurements reveal that CuO electrodes deposited at 150 SILAR cycles and annealed at 623 K possess a sensitivity of 1017 $\mu AmM^{-1}\ cm^{-2}$ with a linear response of 3 µM to 3 mM. The electrochemical analysis for the biosensing study indicates that the CuO electrode is helpful for biosensor device fabrication.

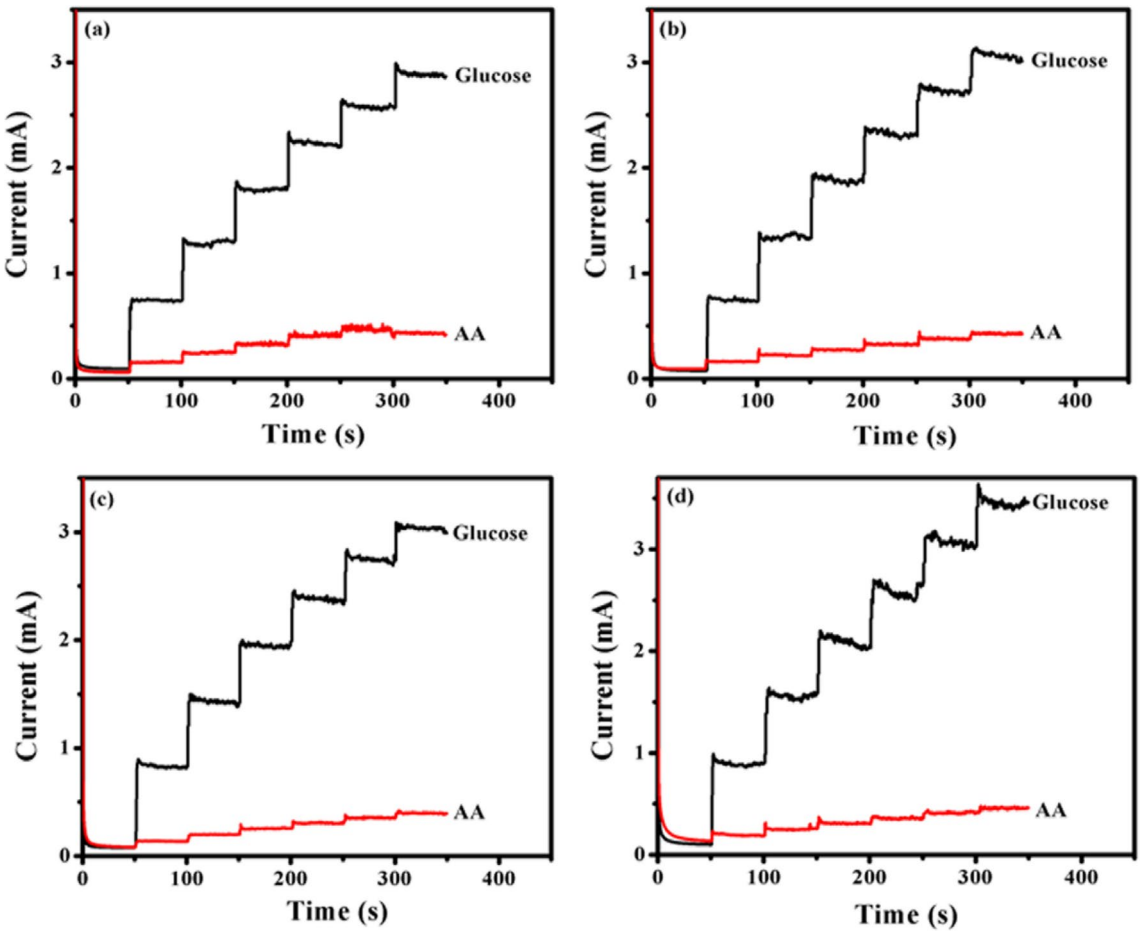

Fig. 8 Amperometric response to glucose as well as Ascorbic acid of CuO with **a** 130 cycles **b** 140 cycles **c** 150 cycle **d** 160 cycles

Acknowledgements The authors are very much thankful for the financial support through DST-PURSE Phase-II (2018-2022) and UGC DSA-Phase II (2018-2023). The Physics Instrumentation Facility Centre (PIFC), Department of Physics, Shivaji University, is greatly acknowledged for providing characterization facilities.

References

1. C. Chen, Q. Xie, D. Yang, H. Xiao, Y. Fu, Y. Tan, S. Yao, Recent advances in electrochemical glucose biosensors: a review. RSC Adv. **3**, 4473–4491 (2013)
2. C. He, J. Liu, Q. Zhang, C. Wu, A novel stable amperometric glucose biosensor based on the adsorption of glucose oxidase on poly(methyl methacrylate)-bovine serum albumin core-shell nanoparticles. Sens. Actuators, B Chem. **166–167**, 802–808 (2012)
3. H. Deng, A.K.L. Teo, Z. Gao, An interference-free glucose biosensor based on a novel low potential redox polymer mediator. Sens. Actuators B **191**, 522–528 (2014)
4. X. Lin, Y. Ni, S. Kokot, Electrochemical mechanism of eugenol at a Cu doped gold nanoparticles modified glassy carbon electrode and its analytical application in food samples. Electrochim. Acta. **133**, 484–491 (2014)
5. D. Ye, G. Liang, H. Li, J. Luo, S. Zhang, H. Chen, J. Kong, A novel non-enzymatic sensor based on CuO nanoneedle/graphene/carbon nanofiber modified electrode for probing glucose in saliva. Talanta **116**, 223–230 (2013)
6. S. Park, H. Boo, T.D. Chung, Electrochemical non-enzymatic glucose sensors. Anal. Chim. Acta. **556**, 46–57 (2006)
7. K. Khun, Z.H. Ibupoto, X. Liu, V. Beni, M. Willander, The ethylene glycol template assisted hydrothermal synthesis of Co_3O_4 nanowires; Structural characterization and their application as glucose non-enzymatic sensor. Mater. Sci. Eng. B **194**, 94–100 (2015)
8. Y. Zhong, T. Shi, Z. Liu, S. Cheng, Y. Huang, X. Tao, G. Liao, Z. Tang, Ultrasensitive non-enzymatic glucose sensors based on different copper oxide nanostructures by in-situ growth. Sens. Actuators, B Chem. **236**, 326–333 (2016)
9. S. Liu, B. Yu, T. Zhang, A novel non-enzymatic glucose sensor based on NiO hollow spheres. Electrochim. Acta. **102**, 104–107 (2013)
10. X. Cao, N. Wang, A novel non-enzymatic glucose sensor modified with Fe_2O_3 nanowire arrays. Analyst **136**, 4241–4246 (2011)
11. J. Wang, W. De Zhang, Fabrication of CuO nanoplatelets for highly sensitive enzyme-free determination of glucose. Electrochim. Acta. **56**, 7510–7516 (2011)
12. Q. Zhang, K. Zhang, D. Xu, G. Yang, H. Huang, F. Nie, C. Liu, S. Yang, CuO nanostructures: synthesis, characterization, growth mechanisms, fundamental properties, and applications. Prog. Mater. Sci. **60**, 208–337 (2014)

13. N. Mukherjee, B. Show, S.K. Maji, U.M.S.K. Bhar, B.C. Mitra, G.G. Khan, A. Mondal, CuO nano-whiskers: electrodeposition, Raman analysis, photoluminescence study and photocatalytic activity. Mater. Lett. **65**, 3248–3250 (2011)
14. F. Bayansal, B. Sahin, M. Yksel, N. Biyikli, H.A. Cetinkara, H.S. Gder, Influence of coumarin as an additive on CuO nanostructures prepared by successive ionic layer adsorption and reaction (SILAR) method. J. Alloys Compd **566**, 78–82 (2013)
15. A.S. Patil, G.M. Lohar, V.J. Fulari, Structural, morphological, optical and photoelectrochemical cell properties of copper oxide using modified SILAR method. J. Mater. Sci. Mater. Electron. **27**, 9550–9557 (2016)
16. H. Qin, Z. Zhang, X. Liu, Y. Zhang, J. Hu, Room-temperature ferromagnetism in CuO sol-gel powders and films. J. Magn. Magn. Mater. **322**, 1994–1998 (2010)
17. F.P. Albores, W.A. Flores, P.A. Madrid, E.R. Valdovinos, M.V. Zapata, F.P. Delgado, M.M. Yoshida, Growth and microstructural study of CuO covered ZnO nanorods. J. Cryst. Growth **351**, 77–82 (2012)
18. J. Xu, K. Yu, J. Wu, D. Shang, L. Li, Y. Xu, Z. Zhu, Synthesis, field emission and humidity sensing characteristics of honeycomb-like CuO. J. Phys. D Appl. Phys. **42**, 075417–075424 (2009)
19. M. Vila, C.D. Guerra, J. Piqueras, Optical and magnetic properties of CuO nanowires grown by thermal oxidation. J. Phys. D Appl. Phys. **43**, 135403–135409 (2010)
20. J.K. Feng, H. Xia, M.O. Lai, L. Lu, Electrochemical performance of CuO nanocrystal film fabricated by room temperature sputtering. Mater. Res. Bull. **46**, 424–427 (2011)
21. A.S. Patil, M.D. Patil, G.M. Lohar, S.T. Jadhav, V.J. Fulari, Supercapacitive properties of CuO thin films using modified SILAR method. Ionics **23**, 1259–1266 (2017)
22. I. Singh, R.K. Bedi, Studies and correlation among the structural, electrical and gas response properties of aerosol spray deposited self assembled nanocrystalline CuO. Appl. Surf. Sci. **257**, 7592–7599 (2011)
23. G. He, L. Wang, One-step preparation of ultra-thin copper oxide nanowire arrays/copper wire electrode for non-enzymatic glucose sensor. Ionics **24**, 3167–3175 (2018)
24. Y. Zhang, Y. Liu, L. Su, Z. Zhang, D. Huo, C. Hou, Y. Lei, CuO nanowires based sensitive and selective non-enzymatic glucose detection. Sens. Actuators B Chem. **191**, 86–93 (2014)
25. Z. Yang, J. Feng, J. Qiao, Y. Yan, Q. Yu, K. Sun, Copper oxide nanoleaves decorated multi-walled carbon nanotube as platform for glucose sensing. Anal. Methods **4**, 1924–1926 (2012)
26. E. Reitz, W. Jia, M. Gentile, Y. Wang, Y. Lei, CuO nanospheres based non-enzymatic glucose sensor. Electroanalysis **20**, 2482–2486 (2008)
27. R.S. Reddy, A. Sreedhar, A.S. Reddy, S. Uthanna, Effect of film thickness on the structural morphological and optical properties of nanocrystalline ZnO films formed by RF magnetron sputtering. Adv. Mater. Lett. **3**(3), 239–245 (2012)
28. H.D. Shelke, A.C. Lokhande, V.S. Raut, A.M. Patil, J.H. Kim, C.D. Lokhande, Facile synthesis of Cu2SnS3 thin films grown by SILAR method: effect of film thickness. J. Mater. Sci.: Mater. Electron. **28**(11), 7912–7921 (2017)
29. S.K. Shinde, V.J. Fulari, D.Y. Kim, N.C. Maile, R.R. Koli, H.D. Dhaygude, G.S. Ghodake, Chemical synthesis of flower-like hybrid $Cu(OH)_2$/CuO electrode: application of polyvinyl alcohol and triton X-100 to enhance supercapacitor performance. Coll. Surf. B Biointerfaces **156**, 165–174 (2017)
30. H. Siddiqui, M.S. Qureshi, F.Z. Haque, Biosynthesis of flower-shaped CuO nanostructures and their photocatalytic and antibacterial activities. Nano-Micro Lett. **12**, 1–11 (2020)
31. G.M. Lohar, S.T. Jadhav, M.V. Takale, R.A. Patil, Y.R. Ma, M.C. Rath, V.J. Fulari, Photoelectrochemical cell studies of Fe^{2+} doped ZnSe nanorods using the potentiostatic mode of electrodeposition. J. Coll. Interface Sci. **458**, 136–146 (2015)
32. G.M. Lohar, S.T. Jadhav, H.D. Dhaygude, M.V. Takale, R.A. Patil, Y.R. Ma, M.C. Rath, V.J. Fulari, Studies of properties of Fe^{3+} doped ZnSe nanoparticles and hollow spheres for photoelectrochemical cell application. J. Alloys Compd. **653**, 22–31 (2015)
33. M. Abdelaziz, E.M. Abdelrazek, Effect of dopant mixture on structural, optical and electron spin resonance properties of polyvinyl alcohol. Phys. B Condens. Matter. **390**, 1–9 (2007)
34. Y. Xu, D. Chen, X. Jiao, Fabrication of CuO pricky microspheres with tunable size by a simple solution route. J. Phys. Chem. B **109**, 13561–13566 (2005)
35. D.P. Dubal, G.S. Gund, C.D. Lokhande, R. Holze, CuO cauliflowers for supercapacitor application: novel potentiodynamic deposition. Mater. Res. Bull. **48**, 923–928 (2013)
36. H. Siddiqui, M.R. Parra, M.M. Malik, F.Z. Haque, Structural and optical properties of Li substituted CuO Nanoparticles. Opt. Quant. Electron. **50**, 1–13 (2018)
37. Z. Changqiong, P. Matthew, Seed layer-assisted chemical bath deposition of CuO films on ITO-coated glass substrates with tunable crystallinity and morphology. Chem. Mater. **26**, 2960–2966 (2014)
38. W.G. Pell, B.E. Conway, Voltammetry at a de Levie brush electrode as a model for electrochemical supercapacitor behaviour. J. Electroanal. Chem. **500**, 121–133 (2001)
39. X. Wang, C. Hu, H. Liu, G. Du, X. He, Y. Xi, Synthesis of CuO nanostructures and their application for non-enzymatic glucose sensing. Sens. Actuators, B Chem. **144**, 220–225 (2010)
40. X.M. Miao, R. Yuan, Y.Q. Chai, Y.T. Shi, Y.Y. Yuan, Direct electrocatalytic reduction of hydrogen peroxide based on nafion and copper oxide nanoparticles modified Pt electrode. J. Electroanal. Chem. **612**, 157–163 (2008)
41. P. Salazar, V. Rico, R.R. Amaro, J.P. Espinos, A.R.G. Elipe, New copper wide range nanosensor electrode prepared by physical vapor deposition at oblique angles for the non-enzimatic determination of glucose. Electrochim. Acta. **169**, 195–201 (2015)
42. X. Zhang, S. Sun, J. Lv, L. Tang, C. Kong, X. Song, Z. Yang, Nanoparticle-aggregated CuO nanoellipsoids for high-performance non-enzymatic glucose detection. J. Mater. Chem. A **2**, 10073–10080 (2014)
43. R. Ahmad, N. Tripathy, Y.B. Hahn, A. Umar, A.A. Ibrahim, S.H. Kim, A robust enzymeless glucose sensor based on CuO nanoseed modified electrodes. Dalt. Trans. **44**, 12488–12492 (2015)
44. J. Chen, W. De Zhang, J.S. Ye, Non-enzymatic electrochemical glucose sensor based on MnO_2/MWNTs nanocomposite. Electrochem. Commun. **10**, 1268–1271 (2008)